

Novel Photo-Detectors and Photo-Detector Systems

M. Danilov

*Institute of Theoretical and Experimental Physics,
B.Cheremushkinskaya 25, 117218 Moscow, Russia
e-mail danilov@itep.ru*

Abstract

Recent developments in photo-detectors and photo-detector systems are reviewed. The main emphasis is made on Silicon Photo-Multipliers (SiPM) - novel and very attractive photo-detectors. Their main features are described. Properties of detectors manufactured by different producers are compared. Different applications are discussed including calorimeters, muon detection, tracking, Cherenkov light detection, and time of flight measurements.

Key words:

SiPM, APD, photo-diode, photo-detector, calorimeter, scintillator

1. From PMT to SiPM

Vacuum Photo-Multipliers (PMTs) are the most popular photo-detectors. They have high sensitivity, single photo-electron resolution, high counting rate, large area, good time resolution. There is an enormous experience in PMT applications in different fields. However PMTs have also drawbacks: sensitivity to magnetic field, large size and low granularity, low quantum efficiency (QE), need of high voltage. They are also quite expensive. These drawbacks can be partially cured. Multi-anode PMTs (MAPMT) offer higher granularity. Micro Channel Plate PMT can work to some extent in magnetic fields. Recently PMTs with high (50%) quantum efficiency have been developed [1].

However, only solid state detectors can provide a cardinal solution of the problems. They are insensitive to magnetic field and compact. They have very high quantum efficiency and granularity. Solid state photo-detectors can be much cheaper than PMTs.

The simplest photo-detector is a PIN photo-diode. It has no amplification and therefore it is very stable. PIN photo-diodes have a high ($\sim 80\%$) QE well matched to the CsI(Tl) emission spectrum which peaks at $\lambda \sim 550$ nm. Therefore they have been used in large quantity in many calorimeters including CLEO, BELLE, BaBar, and GLAST. However a thick ($\sim 300 \mu\text{m}$) sensitive layer leads to a large Nuclear Counting Effect. Charged particles crossing the sensitive layer produce a large number of electron-hole pairs and mimic a large energy deposition in a scintillator. Absence

of amplification prevents usage of PIN photo-diodes with low light yield scintillators.

These two problems are solved in Avalanche Photo Diodes (APD). In APD photo-electrons (p.e.) are produced in a thin ($\sim 6 \mu\text{m}$) sensitive layer amplified in avalanches at a p-n junction. About 120 thousand APDs are used in the CMS calorimeter[2]. Excellent resolution has been achieved in spite of a low photon yield of PbWO₄ crystals. Because of avalanche amplification APDs have a large Excess Noise Factor (ENF) which grows with the amplification. Voltage and temperature sensitivities of the amplification also grow with the amplification. Therefore it is difficult to operate APDs at amplifications above a few hundred.

At a high over-voltage (ΔV) the avalanche amplification transforms into a Geiger discharge. In this mode a photo-diode response does not depend on a number of initial photo-electrons. However it is possible to restore the proportionality of the response to the initial number of p.e. by splitting a photo-diode into a large number of independent pixels connected to the same output. The number of fired pixels is proportional to the number of initial p.e. as long as it is small in comparison with the total number of pixels in a photo-diode. For larger signals the response becomes nonlinear and saturates at the total number of pixels in the photo-diode. Such multi-pixel photo-diodes working in the Geiger mode have been developed in Russia[3]. Now they are produced by many companies which use different names for their products: SiPM, MRS APD, MPPC, MAPD, etc. We will use a generic name SiPM for all of them.

2. SiPM properties

We will discuss SiPM properties using as an example the MEPhI-Pulsar (MEPhI) SiPM. There is by far the largest experience in using such SiPMs in real experiments. About 8 thousand of them were used in the CALICE hadron calorimeter prototype for ILC[4,5] which was tested during the last 3 years at CERN and FNAL.

MEPhI SiPM is a matrix of 1156 pixels with the size $32 \times 32 \mu\text{m}^2$. The SiPM sensitive area is $1.1 \times 1.1 \text{mm}^2$. The pixels have individual polysilicon quenching resistors of a few $M\Omega$ necessary to break off the Geiger discharge. SiPMs are reversely biased with a voltage of about 50V which is about 3V higher than the breakdown voltage (V_{BD}).

2.1. Gain and Photon Detection Efficiency

SiPM gain (G) is determined by a charge released in one pixel discharge which is proportional to a pixel capacitance (C) and ΔV : $Q = \Delta V \times C$. Typical values of $\Delta V \sim 3 \text{V}$ and $C \sim 50 \text{fF}$ lead to $Q \sim 150 \text{fC}$. So one p.e. produces a signal of about 10^6 electrons. This is very similar to a usual PMT. The relative gain variation $\Delta G/G$ is proportional to the relative ΔV variation. Therefore SiPMs operated at smaller ΔV 's like Hamamatsu MPPCs have larger gain sensitivity to the voltage variation and require a better voltage stabilization. A decrease of temperature by 2°C leads to the decrease of the breakdown voltage of the MEPhI SiPM by $\sim 0.1 \text{V}$ and hence to the increase of the gain. Therefore it is desirable to keep temperature variations small.

Photon Detection Efficiency (PDE) is a product of QE , a geometrical efficiency (ϵ), and a probability for a charge carrier to initiate the Geiger discharge (P_G): $PDE = QE \times \epsilon \times P_G$. QE is about 80% at $\lambda = 500 \text{nm}$. The geometrical efficiency is a fraction of a SiPM area which is sensitive. It decreases with the decrease of a pixel size since the area of separating borders between pixels grows. The geometrical efficiency of modern SiPMs can be as large as 70% for $50 \mu\text{m}$ pixels. The probability of the Geiger discharge increases with the ΔV . It grows almost linearly at small ΔV 's but then saturates. This leads to a similar behavior of PDE .

Electrons have a much higher probability to trigger the Geiger discharge in the p-n junction than holes. Therefore SiPMs with a n-p structure are more sensitive to a green light than to a blue light. A blue light (green light) is absorbed in the n-layer (p-layer); the carriers which move to the p-n junction are holes (electrons) and the probability to trigger the discharge is low (high). In order to increase the sensitivity for blue light the n-layer should be made as thin as possible. Another possibility is to use a p-n structure. Fig. 1 shows examples of PDE spectral dependence for different SiPMs[6].

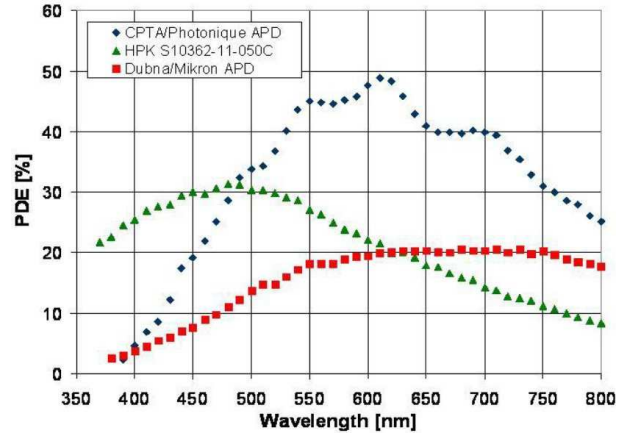


Fig. 1. A photon detection efficiency for different SiPMs.

2.2. After-pulses and cross-talk

Some electrons and holes produced in the discharge can be trapped and then released when the discharge is already quenched. This leads to after-pulses if the pixel has sufficient time to recharge (see Fig. 2[7]). The after-pulses which

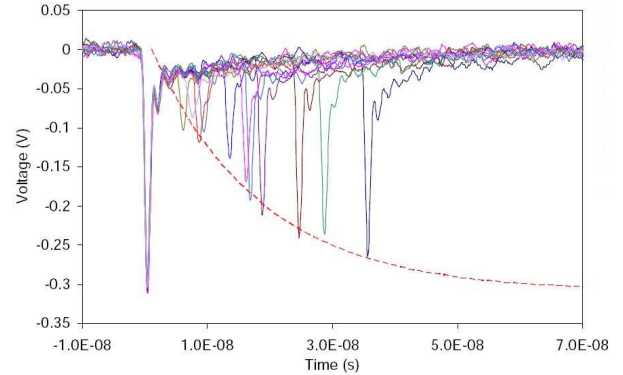


Fig. 2. Examples of after-pulses with different delays.

come soon after the initial signal have smaller amplitudes (see Fig.2) since the pixel voltage is not completely restored. Majority of after-pulses come soon after the initial signal with a decay time of about 18ns[8]. However there is also a fraction with a longer decay time $\sim 90 \text{ns}$. The decay times become shorter at higher temperatures[8]. The after-pulse probability is proportional to the number of electrons in the discharge (i.e. to the gain) and the probability to trigger the Geiger discharge. Therefore it grows roughly as the second power of the ΔV .

The pixel recovery time depends on the pixel capacitance and quenching resistor (R). It can not be much smaller than 100 ns since the quenching resistor can not be small. For such small recovery times the pixel can be fired more than once during a long light pulse coming for example from a scintillator. This increases the dynamic range of a SiPM. However it also makes the response dependent on the shape of the light pulse. This complicates the calibration procedures. Majority of SiPM types have longer recovery time $\sim 1 \mu\text{s}$. The SiPM dead time is much smaller since the

number of pixels is large. Therefore SiPMs can tolerate high counting rates. An LED signal was well seen in a scintillator strip with a SiPM readout when we irradiated it with a ^{90}Sr source up to a counting rate of 600 kHz ($I = 3\mu\text{A}$).

Photons are created in the Geiger discharge with a rate of $\sim 3 \times 10^{-5}$ /electron at $\lambda < 1.1\mu\text{m}$ [9]. Low energy photons have a long absorption length up to $\sim 1\text{ mm}$ at $\lambda = 1.1\mu\text{m}$ and can produce p.e. in neighboring pixels. This leads to the inter-pixel cross-talk. Photo-electrons can be produced in the pixel active region or in the bulk. Therefore there is a prompt and delayed component in the cross-talk[10]. The prompt component can be suppressed by trenches between pixels. The delayed component can be suppressed by an additional p-n junction. This is nicely demonstrated by the MEPhI-MPI (Munich) group. Such double cross-talk suppression allowed them to reduce the cross talk to below 1% level at the amplification of $\sim 2 \times 10^7$ [10]. Modern industrially produced SiPMs have cross-talk values at working ΔV s of 5-10%. The cross talk and after-pulses lead to the increase of ENF which is however still much closer to 1 than in APD or even PMT.

2.3. SiPM response

The SiPM response is a product of several factors. For small light pulses it is given by

$$A = G \times N_\gamma \times PDE \times (1 + XT) \times (1 + AP),$$

where XT is the cross-talk probability, and AP is the after-pulse probability multiplied by the average after-pulse amplitude suppression. For large light signals the saturation due to limited number of pixels becomes important. Since the PDE , G , XT , and AP all grow with ΔV , the SiPM response grows very non-linearly. Fig. 3 shows MEPhI SiPM parameter dependence on the bias voltage. The MEPhI SiPM response at the working point selected for the CALICE application varies by 6%/0.1 V and $-3.5\%/^\circ\text{C}$ [11]. At higher ΔV the sensitivity of the SiPM response to variations of the bias voltage and temperature is weaker.

2.4. Dark rate

SiPMs have a quite high dark rate originating from charge carriers thermally created in the sensitive volume. The typical dark rate is 1-2MHz/mm² at room temperature. The dark rate decreases by a factor of 2 with the temperature decrease by 8°C. Hamamatsu SiPMs have considerably smaller dark rate. The dark rate grows linearly with the ΔV because of the increase in the probability for charge carriers to trigger the Geiger discharge.

2.5. Time resolution

The SiPM response is intrinsically very fast due to a very fast Geiger discharge development in a thin ($\sim 1\text{-}2\mu\text{m}$) depletion layer. The single p.e. timing resolution of about

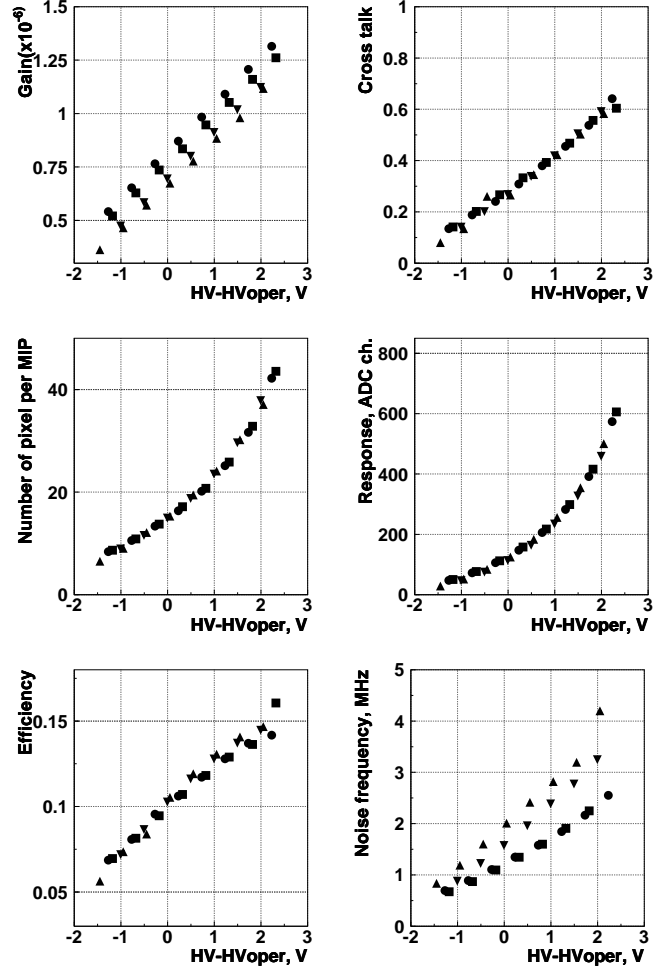


Fig. 3. MEPhI SiPM parameter dependence on bias voltage. Different symbols correspond to 4 randomly selected SiPMs.

0.1ns has been observed[12]. The timing resolution improves as $1/\sqrt{N_{p.e.}}$.

2.6. Insensitivity to magnetic field

SiPMs are not sensitive to a magnetic field. This was tested up to 4T for the MEPhI SiPMs. The SiPM response, gain, cross-talk, and noise frequency did not change in the magnetic field within the measurement accuracy[13]. This feature is extremely important for many SiPM applications.

2.7. Radiation hardness

The SiPM dark current grows linearly with the particle flux as in other Silicon detectors[14]. However, since the initial single photoelectron resolution of SiPMs is by far better than that of say APD, it starts to suffer earlier. The radiation induced dark current in a SiPM is described by the following formula:

$$I = K \cdot F \cdot D \cdot G \cdot P_G \cdot (1 + XT) \cdot (1 + AP) \cdot S \cdot \epsilon \cdot L_{eff},$$

where F is the particle flux, $K = 6 \times 10^{-17}\text{A/cm}$ [15], S is a SiPM area, L_{eff} is the effective thickness from which

charge carriers are collected, D is the energy dependent conversion factor of radiation damage of different particle species to that of 1 MeV neutrons. Fig.4 shows the dark current dependence on proton fluence for MEPhI and CPTA-149 SiPMs at the same PDE ($\sim 10\%$) for the green light. The CPTA detectors show about 2 times smaller current

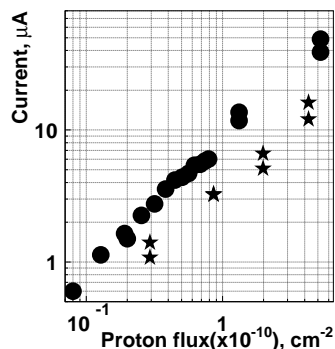


Fig. 4. The dark current increase with the proton flux for MEPhI SiPMs (200 MeV protons, circles) and CPTA MRS-APD (80 MeV protons, stars) operated at the same PDE . Each star corresponds to a different MRS-APD measured after about 1 day after the irradiation. Circles below 10^{10} flux show the current of one SiPM measured online. Other circles correspond to different SiPM samples measured about 1 day after the irradiation.

increase. Moreover they were irradiated with 80MeV protons which have $D \sim 2$ while the MEPhI SiPMs were irradiated with 200MeV protons which have $D \sim 1$. Therefore the effective thickness of the sensitive layer derived from this measurements is 5 times smaller for the CPTA detector. It is about $5\mu\text{m}$ while the MEPhI SiPM has $L_{eff} \sim 25\mu\text{m}$. One can conclude that the CPTA MRS-APD is less vulnerable to the radiation damage. However, if one operates the CPTA MRS-APD at $PDE=30\%$ the dark current increases even a bit faster than in the MEPhI SiPM.

The annealing effect at a room temperature after the proton irradiation is small. The current drops by about 35% in 30 days after the irradiation with 5×10^{10} protons/cm² with $E=80\text{MeV}$. Relative annealing speed does not depend on the dose up to this flux which is equivalent to 10^{11} 1 MeV neutrons/cm².

When the dark current reaches $\sim 5\mu\text{A}$ individual photoelectron peaks in the SiPM response become smeared. However SiPM can be operated at much higher currents.

It was demonstrated[16] that the gain, PDE , V_{BD} , R , and a pixel recovery time of SiPMs do not change after the irradiation with $10^{10}/\text{cm}^2$ protons with $E=82\text{MeV}$ which is equivalent to $2 \times 10^{10}/\text{cm}^2$ of 1 MeV neutrons. This was checked for 5 types of SiPMs from different producers.

SiPMs are less sensitive to electromagnetic radiation. For example 10 SiPMs from MEPhI, CPTA, and Hamamatsu were irradiated with a ^{60}Co Source[11]. All 10 were still operational after 200krad irradiation. The dark current of 1600 pixel MPPC(11-025M) increased considerably after the irradiation but dropped to reasonably small values after annealing at a room temperature (see Fig.5[11]). The

dark current was smaller ($1-3\mu\text{A}$ after 500krad) for 9 other SiPMs including 400 pixel MPPC(S10362-11-050U). They were operational even after a 600 kRad dose. The reason for the fast increase of the current in 1600 pixel MPPC is not clear. One should keep in mind that only one sample was irradiated and more systematic tests are needed. The large dependence of the radiation hardness on the SiPM type (if confirmed) would require detailed radiation studies for each SiPM type.

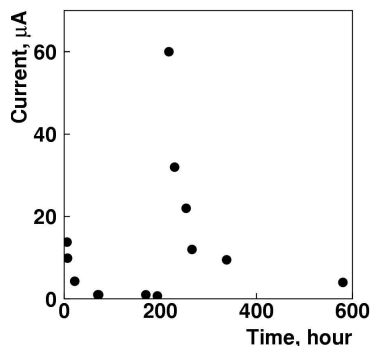


Fig. 5. The dark current of 16000 pixel MPPC irradiated with a ^{60}Co source at $t=0$ (200kRad) and $t=200$ hours (200 kRad).

2.8. Long term stability

The CALICE Hadronic calorimeter with 7620 MEPhI SiPMs has been operated at CERN and FNAL during more than 6 months. We have not observed any increase in the number of dead SiPMs within the measurement uncertainty of about 0.1%. We also have not observed any major change in the SiPM parameters. However a more quantitative analysis of their performance is still to be performed.

2.9. Comparison of SiPMs used in mass applications

So far SiPMs from 3 producers have been used in quantity for experiments: MEPhI SiPMs (CALICE Hadronic calorimeter[4,5]), Hamamatsu MPPCs (CALICE Electromagnetic calorimeter[17]) and CPTA MRS APDs (ALICE TOF test set-up[18]). Properties of these photo-detectors are compared in Fig. 6[11]. $PDEs$ were measured for the plastic scintillator (2.5% PTP and 0.1% POPOP) and the Kuraray Y11 WLS fiber emission spectra. They are labeled as efficiencies for “blue” and “green” light. $PDEs$ of MPPC and MRS APD are very similar for the green light. They are considerably higher than the PDE of the MEPhI SiPM. The blue enhanced MRS APD has the PDE similar to MPPC one but it has much higher dark noise rate. The cross-talk is comparable in the 1600 pixel MPPC and MRS APD. It is much higher in the MEPhI SiPM and 400 pixel MPPC. So the MEPhI SiPM has worse parameters than the more modern MPPC and MRS APD. Nevertheless it was already adequate for mass applications in calorimetry.

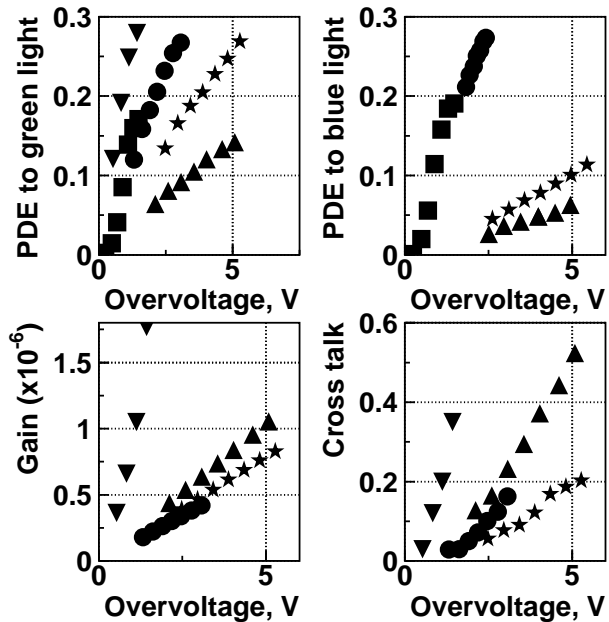


Fig. 6. Parameter dependence on over-voltage for various SiPMs: • - 1600 pixel MPPC; ▼ - 400 pixel MPPC; ▲ - MEPhI-Pulsar SiPM; ★ 556 pixel MRS APD; ■ - $2 \times 2 \text{ mm}^2$ blue sensitive MRS APD.

3. Examples of SiPM applications

3.1. Calorimetry

A small 108 channel hadron calorimeter prototype for the International Linear Collider (ILC) was the first mass application of SiPMs in a real experiment[13]. It consisted of $5 \times 5 \times 0.5 \text{ cm}^3$ scintillator tiles with WLS fiber and MEPhI SiPMs installed directly in the tile. The signals of about 20 p.e./MIP were transported directly without any preamplifier to the LeCroy 2249A ADCs via 25m long coaxial cables. Since there was only very limited experience with SiPMs at that time two identical calorimeters with different photo-detectors were tested simultaneously. One of them used a well established technique of MAPMTs. Another one was based on a relatively new APD readout. All three calorimeters demonstrated adequate and practically identical performance. Results from the calorimeter with the novel SiPM read-out were obtained first because the calibration was based on the response measurements using the distance between signals with different number of p.e. which are well resolved by SiPMs[13]. Results from the calorimeter with MAPMT readout were obtained also fast[13]. Analysis and calibration of the APD data took much longer[19]. The very encouraging experience with the novel SiPM readout resulted in a selection of SiPMs as a baseline for the ILC analogue hadron calorimeter.

The CALICE scintillator hadron calorimeter prototype consists of 7620 Scintillator tiles with WLS fibers and MEPhI SiPMs[4,5]. All SiPMs were thoroughly tested before installation into the tiles[11,20]. The bias voltage was

adjusted to get the same number of pixels per MIP. SiPMs which had too large cross-talk or noise, too low gain or fluctuating dark current were rejected. Many other parameters were also measured but they were found to be mainly within the required limits and practically did not result in additional rejection.

The calorimeter was tested during 2006-2008 at CERN and FNAL. It worked very reliably practically without problem during more than 6 months. Only about 1% of SiPMs were not operational. Majority of them were from the initial production when the selection procedure was not yet fully developed. We can conclude that the experience with the first mass use of SiPMs in the real experiment is very encouraging.

The next engineering prototype is being built now[5]. It will have readout chips installed on very compact PCBs inside the active calorimeter layer. The scintillator tiles with WLS fibers will be only 3mm thick in order to minimize the gaps in the absorber. We plan to use CPTA MRS APDs. They have a higher *PDE* and smaller cross-talk than the MEPhI SiPMs used in the present prototype (see Fig.6). The engineering prototype will be scalable for the mass production of a few million channel CALICE hadron calorimeter.

The CALICE collaboration investigates also a possibility to use blue sensitive SiPMs for a direct read-out of scintillator tiles without WLS fibers.

The CALICE scintillator-tungsten electromagnetic calorimeter prototype is based on $1 \times 4.5 \times 0.3 \text{ cm}^3$ scintillator strips with WLS fiber and the Hamamatsu 1600 pixel MPPC[17]. The first prototype with ~ 500 channels was successfully tested at a 6GeV electron beam at DESY. The second prototype with ~ 2000 channels is tested at FNAL. Initial experience is again very encouraging.

3.2. Muon systems

Scintillator strips with WLS fiber and MAPMT readout is a well established technique for muon detection. This technique was successfully used in the MINOS and OPERA neutrino detectors. It was shown that by switching to a SiPM readout one gets more p.e./MIP and simplifies the technique considerably[21,22]. Because of insensitivity to a magnetic field this technique can be used in collider detectors. A new muon and K_L end cap detector is designed now for the SuperBelle experiment. It will consist of 28 thousand scintillator strips up to 3 meter long[23]. We plan to use the CPTA MRS-APDs as the photo-detectors. It will provide more than 10p.e. from the far end of $300 \times 2.5 \times 1 \text{ cm}^3$ scintillator strips and a small noise rate.

The time resolution of about 1ns allows the determination of the coordinate along the strip with about 15cm accuracy. Similar approach can be used for the muon system of the future International Linear Collider[22].

Using two SiPMs per a scintillator tile it is possible to build a muon system with a negligible noise rate. This fea-

ture is very useful for cosmic muon test set-ups. The cosmic ray test set-up for the ALICE TOF system is based on $15 \times 15 \times 1 \text{ cm}^3$ scintillator tiles with the WLS fiber and two MRS APD read out[18]. About 500 MRS APDs (including spare modules) are used in this effectively working system.

3.3. Neutrino and Astro-particle applications

The T2K neutrino oscillation experiment in Japan plans to use SiPMs practically in all subsystems[24]. Altogether about 50 thousand Hamamatsu MPPCs (S10362-13-050C) will be used. More than 30 thousand of them have been already produced and about 15 thousand have been tested. Tested MPPCs show very good uniformity of parameters. The experiment plans to start data taking already in 2009.

SiPM applications in astro-particle physics are discussed in other talks at this conference. I will mention only two examples. The PEBS balloon experiment plans to check an indication of the cosmic positron flux excess due to Dark Matter annihilation. Linear SiPM arrays will be used in the PEBS scintillating fiber tracker[25]. Each tracker plane consists of 5 layers of $250 \mu\text{m}$ diameter scintillating fibers. The tracker will have 55 thousand read-out channels. The 32 channel SiPM linear arrays from Hamamatsu andIRST are tested. About 10 p.e. per MIP have been observed with the Hamamatsu device. This resulted in a $89 \mu\text{m}$ spatial resolution.

The tungsten-scintillator electromagnetic calorimeter will have about 2 thousand $840 \times 8 \times 2 \text{ mm}^3$ scintillator strips with WLS fibers. We plan to use the CPTA MRS APDs for the read-out. We have observed about 10 p.e./MIP in the 2mm thick strips.

The excellent single photon resolution, high quantum efficiency, low mass, and low bias voltage make SiPMs an interesting alternative to standard PMTs in Dark Matter detection in liquid xenon. The interest to this approach increased after the observation of unexpectedly high SiPM efficiency of $\sim 5.5\%$ to Xe UV scintillation light[26]. Unfortunately our measurements give more than an order of magnitude lower efficiency[27]. Nevertheless we continue this R&D but with the wavelength shifters which transform Xe scintillation light into the SiPM sensitivity region.

3.4. Time of Flight and Cherenkov counters

The excellent single p.e. time resolution allows use of SiPMs for Time of Flight measurements. The timing resolution of 32ps has been obtained using a $3 \times 3 \text{ mm}^2$ MEPhi SiPM coupled to a $3 \times 3 \times 40 \text{ mm}^3$ BC143 plastic scintillator[12]. This resolution contains the contribution from the scintillator 1.4ns decay time.

At the first glance SiPMs are not suitable for the detection of individual photons in Cherenkov light rings because of the high noise rate. However beautiful Cherenkov light rings have been observed recently[28]. The number of p.e.

per ring was larger than with MAPMTs. The SiPM noise was reduced using the excellent SiPM timing resolution.

3.5. Medical and other applications

Medical applications of SiPMs are discussed at this Conference by A. Del Guerra[29]. We would like to mention only the conclusion of this talk - SiPMs are the most promising photo-detectors for the Positron Emission Tomography. It is possible to anticipate other applications of SiPMs in medicine.

The compactness, low bias voltage, large output signals due to the Geiger amplification, single photon counting capability, high quantum efficiency, insensitivity to magnetic field, excellent time resolution, and low cost make SiPM attractive for many other application, for example for radiation monitoring, compact dosimeters etc.

4. Conclusions

SiPMs have many advantages over usual PMTs and other Si detectors. Their basic properties are relatively well understood. SiPMs are already produced by many companies. More than 10 thousand SiPMs have already been used in real experiments and demonstrated excellent performance. Several experiments in particle physics plan to use tens of thousand SiPMs each. So in the near future the number of SiPMs used in experiments will be comparable to the number of the used APDs. We anticipate a wide use of SiPMs in other fields in particular in medicine. There is a very fast development of new and better SiPMs. In spite of several limitations like a small sensitive area and a large noise, SiPMs will become one of the most popular photo-detectors.

5. Acknowledgements

We are grateful to many people for useful discussions in particular to A.Akindinov, V.Balagura, B.Dolgoshein, E.Garutti, V.Golovin, S.Klemin, R.Mizuk, Yu.Musienko, P.Pakhlov, E.Popova, V.Rusinov, F.Sefkow, E.Tarkovsky, I.Tikhomirov. It was a pleasure to work together with many co-authors of the studies reported in this paper. This work was supported in part by the grants RFBR1329.2008.2, RFBR08-02-12100, RFBR/Helmholtz HRJRG-002 and SC Rosatom.

References

- [1] D. Renker , INSTR08, Novosibirsk, March 2008.
- [2] P. Hobson, PSD08, Glasgow, September 2008.
- [3] A. Akindinov *et al.*, Nucl. Instr. Meth. **A 387** (1997) 231; G. Bondarenko *et al.*, Nucl. Phys. Proc. Suppl. **61B** (1998) 347; G. Bondarenko *et al.*, Nucl. Instr. Meth. **A 442** (2000) 187; Z. Sadygov *et al.*, Nucl.Instr. and Meth. **A 504** (2003) 301.

- [4] M. Danilov, Nucl. Instr. and Meth. **A 581** (2007) 451.
- [5] F. Sefkow, **PoS PD07:003**, 2006.
- [6] Yu. Musienko *et al.*, **PoS PD07:012**, 2006.
- [7] C. Piemonte, Talk at FNAL, October 2006.
- [8] F. Retiere and A. Vacheret, NDIP08, Aix-les-Bains, June 2008.
- [9] P. Lacaita *et al.*, IEEE Trans. Electron Dev. 40(3) (1993) 557.
- [10] R. Mirzoyan *et al.*, NDIP08, Aix-les-Bains, June 2008.
- [11] E. Tarkovsky, **PoS PD07:013**, 2006.
- [12] B. Dolgoshein *et al.*, Nucl. Instr. and Meth. **A 563** (2006) 368.
- [13] V. Andreev *et al.* Nucl. Instr. and Meth. **A 540** (2005) 368.
- [14] M. Danilov and G. Eigen, SNIC06, pp.0211, Stanford, April 2006.
- [15] See e.g. G. Lindstrom, Nucl. Instr. and Meth. **A 512** (2006) 30.
- [16] Yu. Musienko *et al.*, NDIP08, Aix-les-Bains, June 2008.
- [17] T. Takeshita, ILD Workshop, Cambridge, September 2008.
- [18] A. Akindinov *et al.*, arXiv:0809.3439 [physics.ins-det].
- [19] V. Andreev *et al.* Nucl. Instr. and Meth. **A 564** (2006) 144.
- [20] V. Rusinov, Nucl. Phys. B (Proc. Suppl.) 150 (2006) 253.
- [21] V. Balagura *et al.* Nucl. Instr. and Meth. **A 564** (2006) 590.
- [22] M. Danilov, LCWS04, p.763, Paris, April 2004.
- [23] P. Pakhlov, Super KEKB meetings, KEK, March and July 2008.
- [24] M. Yokoyama *et al.*, NDIP08, Aix-les-Bains, June 2008, arXiv:0807.3145 [physics.ins-det].
- [25] J. Roper, IPRD08, Siena, October 2008.
- [26] E. Aprile *et al.*, Nucl. Instr. and Meth. **A 556** (2005) 215.
- [27] D. Akimov *et al.*, to be submitted to Instr. and Exp. Techniques.
- [28] P. Krizan, INSTR08, Novosibirsk, March 2008.
- [29] A. Del Guerra, PSD08, Glasgow, September 2008.